

## RESEARCH ARTICLE

# Escape jumping by three age-classes of water striders from smooth, wavy and bubbling water surfaces

Victor Manuel Ortega-Jimenez<sup>1,\*</sup>, Lisa von Rabenau<sup>2</sup> and Robert Dudley<sup>1,3</sup>

## ABSTRACT

Surface roughness is a ubiquitous phenomenon in both oceanic and terrestrial waters. For insects that live at the air–water interface, such as water striders, non-linear and multi-scale perturbations produce dynamic surface deformations which may impair locomotion. We studied escape jumps of adults, juveniles and first-instar larvae of the water strider *Aquarius remigis* on smooth, wave-dominated and bubble-dominated water surfaces. Effects of substrate on takeoff jumps were substantial, with significant reductions in takeoff angles, peak translational speeds, attained heights and power expenditure on more perturbed water surfaces. Age effects were similarly pronounced, with the first-instar larvae experiencing the greatest degradation in performance; age-by-treatment effects were also significant for many kinematic variables. Although commonplace in nature, perturbed water surfaces thus have significant and age-dependent effects on water strider locomotion, and on behavior more generally of surface-dwelling insects.

**KEY WORDS:** *Aquarius remigis*, Capillary waves, Dynamic surfaces, Bubbles, Surface roughness

## INTRODUCTION

Smooth water surfaces are rare in nature given the prevalence of diverse environmental factors (e.g. wind, internal flows) causing deformation, even at small shear stresses. Rough aquatic surfaces, in contrast to uneven solid or granular terrain, are prone to rapid scale-dependent changes (Woolf, 2001; Perlin and Schultz, 2000; Schilling and Zessner, 2011). Thus, for small animals that live at the air–water interface, such surface deformations may represent a chronic challenge while engaging in routine transport, as well as in more extreme behaviors such as escape or chasing. Water striders are a diverse group of surface-dwelling, water-walking insects that live on streams, ponds, lakes and coastal and oceanic waters around the world (Spence and Andersen, 1994). Among insects, water striders are also unique because some taxa (*Halobates* spp.) can spend their entire life on the open ocean, where surface conditions can change dramatically (Cheng et al., 2010). Habitat preferences of water striders are influenced by diverse environmental factors, including wind, stream currents and ripples (Spence, 1981; Fairbairn and Brassard, 1988). Drift avoidance on moving currents is especially important for water striders, because living downstream generally correlates with lower availability and quality

of food. For example, adults of *Aquarius remigis* maintain upstream positions at speeds of up to  $10\text{ cm s}^{-1}$  (Fairbairn and Brassard, 1988).

Walking and jumping on water have typically been studied biomechanically on smooth and unperturbed surfaces (Hu et al., 2003), including robotic emulations of water striders (Wu et al., 2011). In contrast, the effects of surface deformation on water strider locomotion are unknown, especially at small spatial scales where capillary waves (Perlin and Schultz, 2000) and bubbles (Woolf, 2001) can be dominant. Furthermore, given that hatchling water striders are approximately one order of magnitude smaller than the adults, we might expect strong age-dependent effects on locomotor performance, given the relatively larger magnitude of surface deformations and associated forces that they might encounter in the wild. To address these possibilities, we conducted laboratory experiments with three age classes of water striders, *Aquarius remigis*, Gerridae (Say 1832), engaged in escape jumps from smooth, wave-dominated and bubble-dominated surfaces, and measured a number of kinematic and energy aspects of their performance. In general, we predicted that younger (and thus smaller) age classes would experience greater impairment for a given surface disturbance, given that their much lower masses yield greater changes in body acceleration for any externally imposed force.

## MATERIALS AND METHODS

### Insects and experimental water surfaces

We studied 10 fifth instar adults (8 females and 2 males), 10 second or third instar larvae (henceforth, juveniles; sex undetermined), and 10 first instar larvae (henceforth, newborns; sex undetermined) of *A. remigis*. Sample sizes were based on availability and were not computed to detect a pre-specified effect. All second to fifth instars were collected using a dipping net from Strawberry Creek on the UC-Berkeley campus between September and November 2013. First instar larvae were raised in the lab from hatched eggs laid by a breeding pair the previous spring. Collected and recently hatched insects were individually placed into small empty plastic cups, and were weighed prior to experiments. Mean values ( $\pm 1$  s.e.m.) for body mass ( $m_b$ ) of adults, juveniles and newborns were  $44\pm 2$ ,  $21\pm 1$  and  $0.27\pm 0.01$  mg, respectively; values for body length ( $l_b$ ) were  $11.8\pm 0.3$ ,  $6.9\pm 0.3$  and  $1.30\pm 0.04$  mm, respectively.

For experiments, each insect was placed individually into a rectangular pool ( $37\times 8\times 6$  cm) made of clear acrylic and filled with tap water to a depth of  $\sim 3$  cm. After habituation of several minutes, we mechanically stimulated the insect by presenting a rod behind the insect ( $20\text{ cm}\times 1\text{ cm}$  diameter) to elicit an escape response without touching the insect or the water surface (see Caponigro and Eriksen, 1976) under one of three randomly selected experimental conditions: a smooth unperturbed surface, a wavy surface and a bubbling surface (Fig. 1). Following measurements under one experimental condition, the insect was returned to its respective plastic cup for several minutes prior to testing under the remaining

<sup>1</sup>Department of Integrative Biology, University of California, Berkeley, CA 94720, USA. <sup>2</sup>Department of Mechanical Engineering, University of California, Berkeley, CA 94720, USA. <sup>3</sup>Smithsonian Tropical Research Institute, Balboa, Republic of Panama.

\*Author for correspondence (ornithopterus@gmail.com)

 V.M.O., 0000-0003-0024-5086

**List of symbols and abbreviations**

$a_m$	average acceleration
$d$	distance
$E$	mass-specific energy expended during the stroke
$E_w$	energy per unit of area for capillary waves
$h$	maximal height
$l_b$	body length
$P$	mass-specific power during the stroke
$R$	roughness parameter
$t_s$	stroke duration
$u_m$	average speed
$u_p$	peak speed
$\alpha$	stroke angle
$\beta$	pitch
$\gamma$	yaw
$\theta$	takeoff angle
$\psi$	roll

two conditions, randomly chosen. The wavy water surface was generated by mechanical vibration of a ping-pong ball mounted via a rod on a vortex mixer (model K-550-G, Scientific Industries, Inc., Bohemia, NY, USA), and positioned beneath the pool in a beveled washer to prevent slipping (see Fig. 1). The vortex mixer was operated at 1500 rpm, with standing waves correspondingly generated at an amplitude of  $1.1 \pm 1$  mm ( $n=45$ ), a wavelength of  $11.1 \pm 0.2$  mm ( $n=45$ ) and a frequency of  $25 \pm 1$  Hz ( $n=45$ ). The bubbling water surface was produced using two 0.5 cm diameter plastic pipes placed 4 cm from each other along the bottom of the pool. Each pipe was perforated by a series of uniform small holes separated by  $\sim 0.3$  cm, and was connected to an air pump (Air Cadet 420-1901; operating pressure of 23 psi). Bubbles thus generated on the water's surface had an average diameter (as measured from a top view and calibrated video recording) of  $2.9 \pm 0.1$  mm ( $n=633$ ; range 0.4–25 mm).

We characterized surface texture for each of the three experimental conditions by the roughness parameter  $R$ , following methods of Luk et al. (1989). We filmed the water surface for each treatment from a top view (at  $250$  frames  $s^{-1}$ ), and analyzed 20 consecutive video frames using MATLAB. After subtracting the stationary background from each image, we calculated the standard

deviation of the gray level distribution (s.d.) and the root mean square height of the gray level distribution (rms);  $R$  is given by the ratio of s.d. to rms. Values of  $R$  for smooth, wave-dominated and bubble-dominated surfaces were  $0.3 \pm 0.1\%$ ,  $4.7 \pm 0.3\%$  and  $8.6 \pm 0.3\%$ , respectively (see Fig. S1).

**Escape kinematics**

We filmed 10 water striders of each age class propelling themselves with a single escape stroke of the middle legs from each of the three experimental water surfaces (and with no contact on the Plexiglas walls); jumps of water striders are conducted by the middle legs alone (Hu et al., 2003). A single camera (AOS X-PRI, operated at  $250$  frames  $s^{-1}$ ) mounted on the top of the pool was used to film a dorsal view of adults and juveniles; this camera also captured a lateral view of the insects as projected onto a mirror positioned laterally at an angle of  $\sim 45$  deg to the pool. Newborns were filmed at  $100$  frames  $s^{-1}$  using two orthogonally oriented video cameras (AOS X-PRI). For three-dimensional calibration and reconstruction, we filmed a physical calibration frame with multiple internal landmarks to obtain direct linear transformation (DLT) coefficients (see Hedrick, 2008; digitization software is available at <https://www.unc.edu/~thedrick/software1.html>). We manually digitized the anterior point of the head, the tip of the abdomen, and the tips and bases of both mid-legs through the stroke. Instantaneous speed  $v_i$  and acceleration  $a_i$  of the head were estimated using the first and second derivatives of a mean square error quintic spline (Walker, 1998). The takeoff angle  $\theta$  was calculated as the angle between horizontal and the vector connecting the longitudinal body midpoint to the head for the two video frames immediately following the end of the mid-leg stroke. The maximal height  $h$  and distance  $d$  attained by the head during the stroke were also measured, as was the stroke angle  $\alpha$ , the angle formed by the two line segments connecting the tip and base of the mid-leg at the beginning and the end of the stroke. Stroke duration  $t_s$  was calculated as the number of frames from the beginning to the end of the stroke, divided by the frame rate. The vector formed by the head and tip of the abdomen was used to calculate body pitch  $\beta$  and yaw  $\gamma$ , using vector projections over the  $x$ - $z$  and  $y$ - $z$  planes, respectively. The vector projection over the  $x$ - $y$  plane formed between the base of the two mid-legs was used to calculate the roll angle  $\psi$ . We normalized height  $h$ , distance  $d$ ,

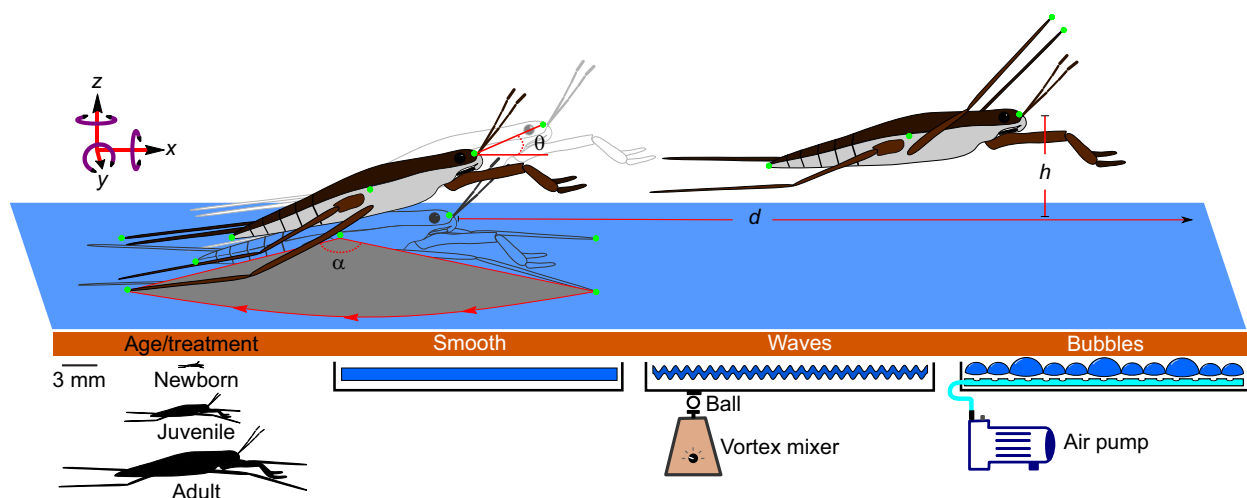


**Fig. 1.** Drawing showing water striders of three age classes (newborns, juveniles and adults) rowing on smooth, wave-dominated and bubble-dominated water surfaces. Green dots represent the digitized points used to calculate kinematic variables. Stroke angle  $\alpha$ , total distance  $d$ , attained height  $h$  and takeoff angle  $\theta$  are shown; see Materials and methods for details.

average speed  $u_m$ , peak speed  $u_p$  and average acceleration  $a_m$  by the body length  $l_b$ . Body mass-specific energy  $E$  and power  $P$  expended during the stroke were calculated as  $0.5 u_p^2$  and  $E/t_s$ , respectively. Raw data can be accessed from the Dryad Digital Repository (Ortega-Jimenez et al., 2017; <http://dx.doi.org/10.5061/dryad.7f0h0>). This research adheres to the ASAB/ABS Guidelines for the Use of Animals in research. No permission was required to collect water striders. The present study did not involve regulated, endangered or protected species.

### Statistics

We applied a mixed-effect ANOVA to tests for differences in age class and treatment in the following variables:  $d$ ,  $u_m$ ,  $u_p$ ,  $a_m$ ,  $h$ ,  $\theta$ ,  $\alpha$ ,  $t_s$ ,  $\beta$ ,  $\gamma$ ,  $\psi$ ,  $E$  and  $P$ . In order to fulfill assumptions of the ANOVA, all variables were transformed with the reciprocal of the square root, the reciprocal of the double square root, or a logarithmic function. Deviations from sphericity were observed in  $d$  and  $u_m$  ( $\epsilon < 0.7$ ), and Greenhouse–Geisser adjustments were applied accordingly. Tukey's test was used for pairwise comparisons. All analyses were conducted in R (v. 3.02, <http://www.R-project.org/>).

### RESULTS

Perturbed water surfaces visibly affected the jumping performance of water striders (Movie 1). Pooling all data, the normalized distance  $d$  reached by water striders in the escape stroke decreased with age and with surface roughness (Fig. 2A, Tables 1 and 2). However, values of  $d$  for adults did not differ significantly among surface modes ( $P > 0.5$  for pairwise contrasts); for juveniles, the normalized distance was significantly reduced by 33% in bubbly conditions compared with the control ( $P = 0.03$ ), and for newborns, the normalized distance was reduced significantly by 44% and 33% for wavy and bubbly surfaces, respectively, in comparison with the smooth surface ( $P < 0.01$  for both pairwise comparisons; see Fig. 2A). Normalized translational speeds, both  $u_m$  and  $u_p$ , and normalized mean acceleration  $a_m$  also decreased with age (Fig. 2B; Tables 1 and 2). Both adults and juveniles exhibited a significant reduction in  $u_p$  on the bubbly surface of ~20% compared with that on smooth water ( $P < 0.01$ ). Newborns showed a significantly decreased  $u_m$  on both wavy (50%) and bubbly surfaces (30%) in comparison with the smooth surface ( $P < 0.05$  in both cases). Also, newborns decreased  $u_p$  by 40% on the wavy surface relative to that on the smooth surface ( $P < 0.001$ ), but showed approximately 3 times higher  $a_m$  when moving on bubbly relative to smooth or wavy

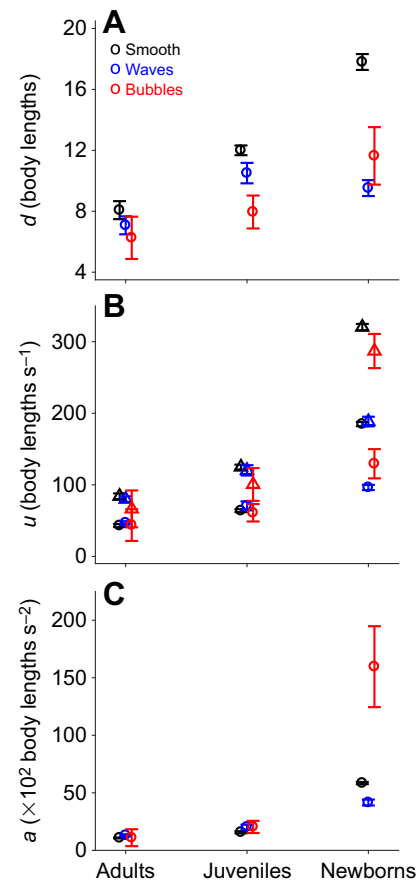


**Fig. 2. Normalized distance, speed and acceleration of three age-classes of water striders rowing on smooth, wave-dominated and bubble-dominated water surfaces.** (A) Distance ( $d$ ). (B) Speed ( $u$ ). (C) Acceleration ( $a$ ). Peak (circles) and average (triangles) values for  $u$  and  $a$  are shown for smooth (black), wave-dominated (blue) and bubble-dominated (red) conditions. Data represent means  $\pm$  s.e.m. The sample size  $n$  for each condition was 10. Each individual was exposed once to each experimental condition. See Results and Table 2 for  $P$ -values.

conditions ( $P < 0.001$ ; see Fig. 2C). Allometrically, translational speeds increased similarly with mass for the three surface conditions, whereas the acceleration actually increased with mass only for the bubble-dominated surface relative to the other conditions (Table 1; Fig. S2).

**Table 1. Kinematic results for adult, juvenile and newborn water striders jumping from three experimental water surfaces**

Treatment	$d$ (body lengths)	$u_m$ (body lengths $s^{-1}$ )	$u_p$ (body lengths $s^{-1}$ )	$a_m$ ( $\times 10^2$ body lengths $s^{-2}$ )	$h$ (body lengths)	$\theta$ (deg)	$\alpha$ (deg)	$t_s$ (ms)	$\beta$ (deg)	$\psi$ (deg)	$\gamma$ (deg)	$E$ ( $\times 10^{-2}$ J $kg^{-1}$ )	$P$ (W $kg^{-1}$ )
<b>Adults</b>													
Smooth	8 $\pm$ 1	43 $\pm$ 2	84 $\pm$ 4	11 $\pm$ 0	0.4 $\pm$ 0.1	10 $\pm$ 1	102 $\pm$ 2	82 $\pm$ 7	5 $\pm$ 1	11 $\pm$ 1	8 $\pm$ 1	49 $\pm$ 3	6.1 $\pm$ 0.4
Wavy	7 $\pm$ 0	47 $\pm$ 2	80 $\pm$ 3	13 $\pm$ 1	0.5 $\pm$ 0.1	13 $\pm$ 2	104 $\pm$ 5	75 $\pm$ 5	8 $\pm$ 1	10 $\pm$ 2	9 $\pm$ 1	45 $\pm$ 3	6.1 $\pm$ 0.5
Bubbling	6 $\pm$ 1	44 $\pm$ 3	66 $\pm$ 5	11 $\pm$ 1	0.8 $\pm$ 0.1	22 $\pm$ 2	93 $\pm$ 4	75 $\pm$ 4	15 $\pm$ 1	13 $\pm$ 2	15 $\pm$ 3	31 $\pm$ 3	4.1 $\pm$ 0.4
<b>Juveniles</b>													
Smooth	12 $\pm$ 1	64 $\pm$ 2	125 $\pm$ 4	16 $\pm$ 1	0.6 $\pm$ 0.1	13 $\pm$ 1	108 $\pm$ 2	73 $\pm$ 2	6 $\pm$ 1	15 $\pm$ 2	7 $\pm$ 1	36 $\pm$ 1	5.0 $\pm$ 0.2
Wavy	11 $\pm$ 1	71 $\pm$ 6	120 $\pm$ 7	20 $\pm$ 2	0.7 $\pm$ 0.1	15 $\pm$ 1	102 $\pm$ 3	68 $\pm$ 3	8 $\pm$ 2	13 $\pm$ 2	16 $\pm$ 4	34 $\pm$ 3	5.0 $\pm$ 0.4
Bubbling	8 $\pm$ 1	61 $\pm$ 4	101 $\pm$ 7	20 $\pm$ 3	1.0 $\pm$ 0.1	22 $\pm$ 2	101 $\pm$ 4	81 $\pm$ 5	10 $\pm$ 1	13 $\pm$ 1	9 $\pm$ 2	24 $\pm$ 3	3.1 $\pm$ 0.4
<b>Newborns</b>													
Smooth	18 $\pm$ 1	185 $\pm$ 22	320 $\pm$ 26	59 $\pm$ 7	0.4 $\pm$ 0.1	5 $\pm$ 1	127 $\pm$ 5	62 $\pm$ 3	9 $\pm$ 1	5 $\pm$ 0	9 $\pm$ 2	9 $\pm$ 1	1.5 $\pm$ 0.2
Wavy	10 $\pm$ 1	96 $\pm$ 12	189 $\pm$ 23	42 $\pm$ 5	0.3 $\pm$ 0.1	7 $\pm$ 2	133 $\pm$ 8	72 $\pm$ 5	10 $\pm$ 1	6 $\pm$ 1	10 $\pm$ 2	3 $\pm$ 1	0.4 $\pm$ 0.1
Bubbling	12 $\pm$ 2	129 $\pm$ 20	287 $\pm$ 24	160 $\pm$ 35	2.8 $\pm$ 0.6	48 $\pm$ 9	135 $\pm$ 19	57 $\pm$ 8	41 $\pm$ 2	77 $\pm$ 10	59 $\pm$ 9	8 $\pm$ 2	1.5 $\pm$ 0.3

Data are presented as means  $\pm$  1 s.e.m.  $d$ , total distance;  $u_m$ , average speed;  $u_p$ , peak speed;  $a_m$ , average acceleration;  $h$ , height;  $\theta$ , takeoff angle;  $\alpha$ , stroke angle;  $t_s$ , stroke duration;  $\beta$ , pitch;  $\psi$ , roll;  $\gamma$ , yaw;  $E$ , mass-specific energy expended during the stroke;  $P$ , mass-specific power during the stroke.  $d$ ,  $u_m$ ,  $u_p$ ,  $a_m$  and  $h$  were normalized by body length.

**Table 2. Results of a mixed-effect ANOVA for kinematic and energetic variables from water striders of three age classes jumping from smooth, wave-dominated and bubble-dominated water surfaces**

Variable	Group	d.f.	<i>F</i>	<i>P</i>
<i>d</i>	Age	2, 27	14.8	<b>&lt;0.001</b>
	Treatment	2, 54	10.5	<b>&lt;0.01</b>
	Age×treatment	4, 54	1.2	0.3
<i>u<sub>m</sub></i>	Age	2, 27	48	<b>&lt;&lt;0.001</b>
	Treatment	2, 54	1.7	0.2
	Age×treatment	4, 54	2.5	0.07
<i>u<sub>p</sub></i>	Age	2, 27	162	<b>&lt;&lt;0.001</b>
	Treatment	2, 54	9	<b>&lt;0.001</b>
	Age×treatment	4, 54	7.4	<b>&lt;0.001</b>
<i>a<sub>m</sub></i>	Age	2, 27	222	<b>&lt;&lt;0.001</b>
	Treatment	2, 54	12	<b>&lt;0.001</b>
	Age×treatment	4, 54	14	<b>&lt;0.001</b>
<i>h</i>	Age	2, 27	3.5	<b>0.044</b>
	Treatment	2, 54	40	<b>&lt;&lt;0.001</b>
	Age×treatment	4, 54	12	<b>&lt;0.001</b>
$\theta$	Age	2, 27	5.7	<b>&lt;0.05</b>
	Treatment	2, 54	67	<b>&lt;&lt;0.001</b>
	Age×treatment	4, 54	11	<b>&lt;0.001</b>
$\alpha$	Age	2, 27	86	<b>&lt;&lt;0.001</b>
	Treatment	2, 54	1.1	0.3
	Age×treatment	4, 54	3	<b>0.03</b>
<i>t<sub>s</sub></i>	Age	2, 27	7	<b>&lt;0.01</b>
	Treatment	2, 54	0.1	0.95
	Age×treatment	4, 54	2.2	0.08
$\beta$	Age	2, 27	48	<b>&lt;&lt;0.001</b>
	Treatment	2, 54	84	<b>&lt;&lt;0.001</b>
	Age×treatment	4, 54	12	<b>&lt;0.001</b>
$\psi$	Age	2, 27	1.6	0.2
	Treatment	2, 54	39	<b>&lt;&lt;0.001</b>
	Age×treatment	4, 54	31	<b>&lt;&lt;0.001</b>
$\gamma$	Age	2, 27	3.9	<b>0.032</b>
	Treatment	2, 54	14.7	<b>&lt;0.001</b>
	Age×treatment	4, 54	8.3	<b>&lt;0.001</b>
<i>E</i>	Age	2, 27	188	<b>&lt;&lt;0.001</b>
	Treatment	2, 54	12	<b>&lt;0.001</b>
	Age×treatment	4, 54	6	<b>&lt;0.001</b>
<i>P</i>	Age	2, 27	175	<b>&lt;&lt;0.001</b>
	Treatment	2, 54	8	<b>&lt;0.001</b>
	Age×treatment	4, 54	9	<b>&lt;0.001</b>

For definitions, see Table 1. *d*, *u<sub>m</sub>*, *u<sub>p</sub>*, *a<sub>m</sub>* and *h* were normalized by body length. Significant *P*-values are shown in bold.

We also found significant differences in body pitch, roll and yaw with age (Fig. 3, Tables 1 and 2). Newborns showed higher values of pitch relative to the two older age groups ( $P < 0.001$  for both pair contrasts). Adults, juveniles and newborns exhibited a higher body pitch (3, 2 and 4 times, respectively) on the bubbly surface than on the smooth surface ( $P < 0.001$  for all three pairwise comparisons). By contrast, only newborns exhibited greater roll and yaw, 77 and 59 deg, respectively, on the bubbly surface relative to smooth water ( $P < 0.001$  for both pairwise comparisons). Height attained and takeoff angle differed significantly with age and treatment, including significant interaction effects (Table 2). Adults, juveniles and newborns exhibited significantly greater heights (2, 2 and 7 times, respectively) and takeoff angles on the bubbly relative to the smooth water surface ( $P < 0.05$  for all comparisons; Fig. 4A,C). Leg stroke angle showed significant variation with age and surface type, whereas stroke duration differed only with age (Table 2). Adults had smaller stroke angles and longer stroke durations than newborns ( $P < 0.01$  for both contrasts). However, there were no significant differences among treatments in either variable for each age class ( $P > 0.5$  for all pair contrasts), except for newborns for

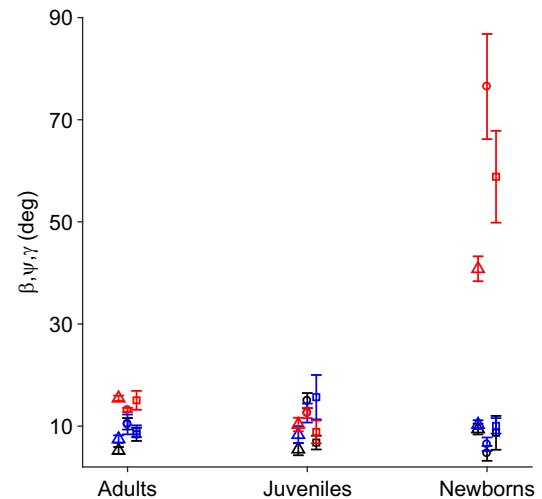


**Fig. 3. Body orientation of three age classes of water striders rowing on smooth, wave-dominated and bubble-dominated water surfaces.** Pitch  $\beta$  (triangles), roll  $\psi$  (circles) and yaw  $\gamma$  (squares) are represented for smooth (black), wave-dominated (blue) and bubble-dominated (red) conditions. Data represent means  $\pm$  s.e.m.,  $n=10$  for each condition. Each individual was exposed once to each experimental condition. See Results and Table 2 for *P*-values.

which stroke angle differed only 6% between the smooth and the bubbly conditions ( $P < 0.01$ ; see Fig. 4B,D).

Finally, mass-specific kinetic energy *E* and mass-specific power *P* during escape increased with age ( $P < 0.001$  for all pairwise comparisons; Fig. 5, Tables 1 and 2). Adults and juveniles had 30–40% lower values of *E* and *P* while escaping on bubbles relative to a smooth surface ( $P < 0.01$  for both comparisons). In contrast, newborns presented 3 times lower *E* and 4 times lower *P* on the wavy relative to the smooth surface ( $P < 0.001$ ; see Fig. 5), given their much reduced velocities during this transient behavior.

## DISCUSSION

Water striders routinely move on perturbed waters (including waves and bubbles) produced by wind fetch, rain and waterfalls, or when encountered in proximity to the complex three-dimensional wakes produced in streams by rocks, vegetation and interaction with the shore. During prey capture, water striders can also experience high-frequency waves produced by insects trapped on the water surface (see Fig. 6). Such millimeter-scale waves and air bubbles on a water surface can impair the escape performance of water striders, and these effects are age dependent. We found that whereas adults were minimally impaired, and juveniles were only moderately affected when jumping from a bubbling surface, newborns experienced a dramatic reduction in performance on both wavy and bubbly surfaces. Ripples and air bubbles are both conspicuous and common on inland and oceanic waters. Capillary and gravity waves, for example, can be generated by low wind speeds (Perlin and Schultz, 2000), light rain (Tsimplis, 1992) and animals moving on the water's surface. Capillary waves (i.e.  $< 10$  mm in amplitude) are smaller than gravity waves, and are quickly dissipated because their decay is a strong function of surface tension (Perlin and Schultz, 2000). The energy per unit of area for capillary waves,  $E_w$ , can be calculated as  $\pi^2 \sigma A^2 / 4 \lambda^2$ , where  $\sigma$  is the water surface tension,  $A$  is wave amplitude and  $\lambda$  is wavelength (see Denny, 1993). For our wave-dominated experimental condition, the corresponding value of  $E_w$  is  $\sim 2 \times 10^{-3}$  N m $^{-1}$  (or alternatively, J m $^{-2}$ ), only 3% of the force per length that is generated by an adult

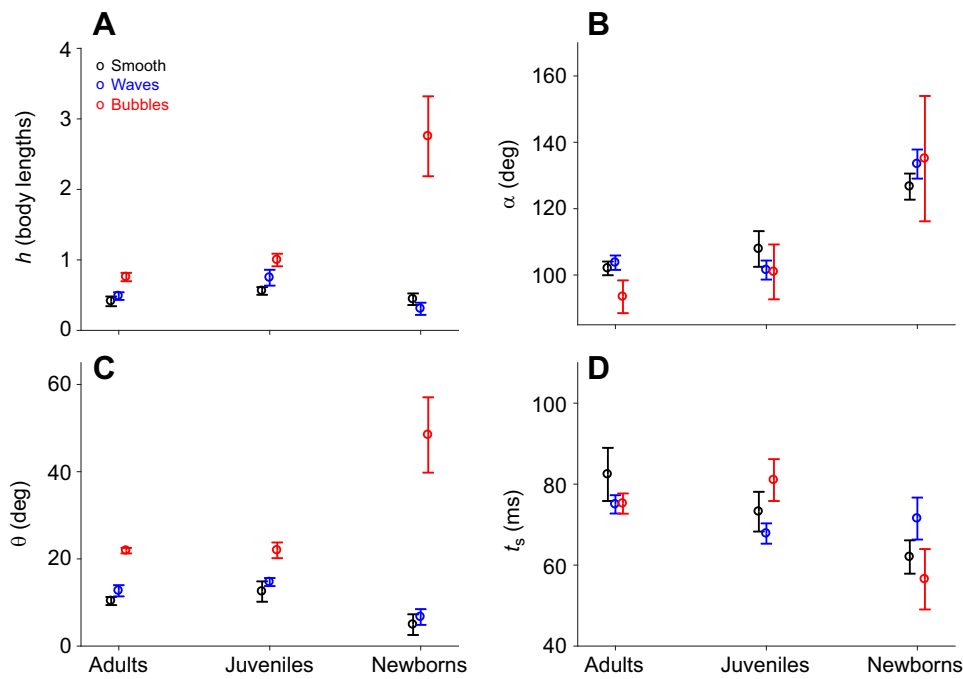


**Fig. 4. Normalized height, stroke angle, takeoff angle and stroke duration for three age classes of water striders moving on smooth, wave-dominated and bubble-dominated water surfaces.** (A) Height ( $h$ ). (B) Stroke angle ( $\alpha$ ). (C) Takeoff angle ( $\theta$ ). (D) Stroke duration ( $t_s$ ). Data represent means  $\pm$  s.e.m.,  $n=10$  for each condition. Each individual was exposed once to each experimental condition. See Results and Table 2 for  $P$ -values.

water strider during a stroke ( $80 \times 10^{-3} \text{ N m}^{-1}$ ; see Hu et al., 2003). By contrast, newborn striders can generate only  $\sim 3 \times 10^{-3} \text{ N m}^{-1}$  during a stroke (Hu et al., 2003), a value comparable to that of our

experimental waves, which, accordingly, were more disruptive relative to jump performance.

Surface waves can also generate bubbly regimes. Air bubbles up to 1 cm in diameter are produced by breaking wind wakes (Deane and Stokes, 2002) and also by raindrop impact on the water surface (Prosperetti and Oguz, 1993). On the oceans, wind stress associated with Langmuir circulation accumulates bands of air bubbles and floating biomaterial (Liang et al., 2012). Cheng et al. (2010) reported that *Halobates* species are commonly found on bubbles at the sea surface, and we have observed adult *A. remigis* walking over and breaking air bubbles on a creek (V.M.O.-J., personal observation). Bubbles can entrap not only gas but also detritus, microorganisms (see Blanchard, 1989) and possibly tiny insects; the last may serve as a source of food for water striders if the bubble can be successfully penetrated and broken. Bubble puncture for feeding or during locomotion may, however, involve some risk. Air bubbles in water are unstable and collapse quickly ( $\sim 10^{-6} \text{ s}$ ), reaching accelerations of more than a thousand times that of gravity (Liger-Belair et al., 2012; Walls et al., 2014). The force per unit length of the spreading rim equals twice that of surface tension, i.e.  $\sim 0.15 \text{ N m}^{-1}$ , whereas adult water striders can generate a force of only  $\sim 0.08 \text{ N m}^{-1}$ . Thus, water striders close to breaking bubbles will be subjected to strong shear stresses that may augment leg impulses during takeoff (e.g. the high speeds and accelerations reached by newborns; see Table 1), and that could be damaging. Moreover, films and jets formed during bubble bursting may irregularly collide with jumping water striders and induce large changes in body pitch, roll and yaw (Fig. 3).

It is important to note that newborns under bubble-dominated conditions may be unable to control their takeoff trajectory when inadvertently propelled by a breaking bubble (e.g. Movie 1). For example, a passive styrofoam ball (radius 15 mm) can be launched horizontally  $\sim 2 \text{ cm}$  by a breaking bubble of comparable size (Movie 2). Surface perturbations impose forces which should, in general, result in greater accelerations for smaller objects. This was the case for water striders escaping only on the bubble-dominated surface (Table 1; Fig. S2), suggesting that both time scale and local geometry of a dynamic surface will influence locomotion. The physical effects of

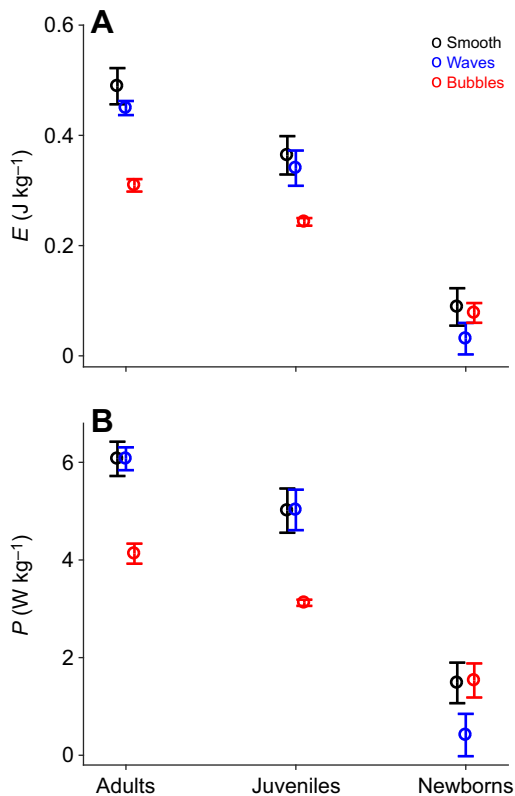


**Fig. 5. Mass-normalized energy and power of three age-classes of water striders moving on smooth, wave-dominated and bubble-dominated water surfaces.** (A) Energy ( $E$ ). (B) Power ( $P$ ). Data represent means  $\pm$  s.e.m.,  $n=10$  for each condition. Each individual was exposed once to each experimental condition. See Results and Table 2 for  $P$ -values.

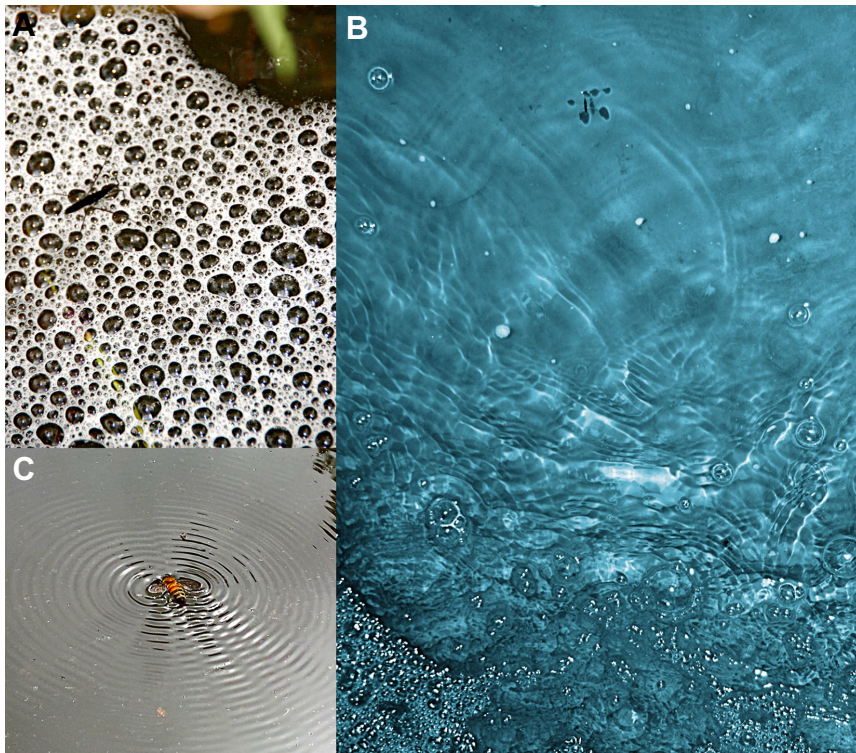


**Fig. 6. Images of insects on perturbed water surfaces.** (A,B) Water strider moving on bubbly (A) and wave-perturbed (B) surfaces in nature. (C) A honeybee trapped in the water's surface, producing waves.

breaking bubbles may be fundamentally different from those of standing waves, for example, on the spatial scales relevant to water striders. This possibility is amenable to analysis with higher temporal resolution cameras than were used here, and may have general consequences for surface-dwelling insects moving on perturbed waters. However, surface deformations could, in some cases, enhance locomotion depending on the timing of the appendage stroke relative to changes in the local surface geometry.

Perturbations on water surfaces have not been quantitatively described or evaluated relative to habitat choice in water striders, but the negative consequences of waves and bubbles documented here may influence the success of escape from various predators, including seabirds (for the pelagic *Halobates*), odonates, fish and backswimmers (see Cheng et al., 2010; Rowe, 1994). Habitat selection by larval instars may be particularly influenced by surface roughness. Water strider development from the initial hatch to the adult stage requires approximately 2 months (Spence and Andersen, 1994). During this time, adults and nymphs of apterous morphs coexist, although in some species there is habitat partitioning between age classes (Vepsäläinen and Jarvinen, 1974), and adults show larger home ranges than juveniles (Wheelwright and Wilkinson, 1985). For example, adults of *Gerris argentatus* are more frequently distributed on open water whereas young nymphs are closer to edges, which may provide refuge from predators or cannibalistic adults (see Vepsäläinen and Jarvinen, 1974; Cárcamo and Spence, 1994). Surface perturbations may also be buffered at the water's edge through wall effects and surrounding vegetation, further motivating habitat association.

In conclusion, we show here strong age-dependent effects on escape performance of water striders jumping from dynamic and complex water surfaces. Physical perturbations such as waves and bubbles are unstudied relative to movement ecology by water striders, and may influence locomotor dynamics and energetics as well as broader features of behavior and habitat choice. Intense

bubbling, as may occur at the base of cascades and waterfalls, may be particularly challenging for water striders. For example, juveniles resident on bubbling surfaces for several minutes sometimes lose hydrophobicity and sink beneath the bubble layer (Movie 3). We suggest that the effects of surface roughness, including waves and bubbles, are far reaching for water striders, and encourage their characterization in natural environments.

#### Acknowledgements

We thank Sarahi Arriaga-Ramirez for her comments and assistance with programming.

#### Competing interests

The authors declare no competing or financial interests.

#### Author contributions

Conceptualization: V.M.O.-J.; Methodology: V.M.O.-J., L.v.R., R.D.; Software: V.M.O.-J.; Validation: V.M.O.-J.; Formal analysis: V.M.O.-J.; Investigation: V.M.O.-J., L.v.R.; Resources: V.M.O.-J., R.D.; Data curation: V.M.O.-J.; Writing - original draft: V.M.O.-J., L.v.R., R.D.; Writing - review & editing: V.M.O.-J., L.v.R., R.D.; Supervision: V.M.O.-J., R.D.

#### Funding

This work was supported by the Department of Integrative Biology, University of California Berkeley.

#### Data availability

Raw data have been deposited in the Dryad Digital Repository: <http://dx.doi.org/10.5061/dryad.7f0h0>

#### Supplementary information

Supplementary information available online at <http://jeb.biologists.org/lookup/doi/10.1242/jeb.157172.supplemental>

#### References

- Blanchard, D. C. (1989). The ejection of drops from the sea and their enrichment with bacteria and other materials: a review. *Estuaries* **12**, 127–139.
- Caponigro, M. A. and Eriksen, C. H. (1976). Surface film locomotion by the water strider, *Gerris remigis* Say. *Am. Midl. Nat.* **95**, 268–278.

- Cárcamo, H. A. and Spence, J. R.** (1994). Kin discrimination and cannibalism in water striders. (Heteroptera: Gerridae): another look. *Oikos* **70**, 412–416.
- Cheng, L., Spear, L. B. and Ainley, D. G.** (2010). Importance of marine insects (Heteroptera: Gerridae, Halobates spp.) as prey of eastern tropical Pacific seabirds. *Mar. Ornithol.* **38**, 91–95.
- Deane, G. B. and Stokes, M. D.** (2002). Scale dependence of bubble creation mechanisms in breaking waves. *Nature* **418**, 839–844.
- Denny, M. W.** (1993). *Air and Water: The Biology and Physics of Life's Media*. Princeton, NJ: Princeton Univ. Press.
- Fairbairn, D. J. and Brassard, J.** (1988). Dispersion and spatial orientation of *Gerris remigis* (Hemiptera, Gerridae) in response to water current: a comparison of pre- and post-diapause adults. *Physiol. Entomol.* **13**, 153–164.
- Hedrick, T. L.** (2008). Software techniques for two- and three-dimensional kinematic measurements of biological and biomimetic systems. *Bioinspir. Biomim.* **3**, 034001.
- Hu, D. L., Chan, B. and Bush, J. W. M.** (2003). The hydrodynamics of water strider locomotion. *Nature* **424**, 663–666.
- Liang, J.-H., McWilliams, J. C., Sullivan, P. P. and Baschek, B.** (2012). Large eddy simulation of the bubbly ocean: new insights on subsurface bubble distribution and bubble-mediated gas transfer. *J. Geophys. Res.* **117**, C04002.
- Liger-Belair, G., Seon, T. and Antkowiak, A.** (2012). Collection of collapsing bubble driven phenomena found in champagne glasses. *Bubble. Sci. Eng. Technol.* **4**, 21–34.
- Luk, F., Huynh, V. and North, W.** (1989). Measurement of surface roughness by a machine vision system. *J. Phys. E Sci. Instrum.* **22**, 977–980.
- Ortega-Jimenez, V. M., von Rabenau, L. and Dudley, R.** (2017). Data from: Escape jumping by three age-classes of water striders from smooth, wavy and bubbling water surfaces. Dryad Digital Repository. <http://dx.doi.org/10.5061/dryad.7f0h0>
- Perlin, M. and Schultz, W. W.** (2000). Capillary effects on surface waves. *Annu. Rev. Fluid Mech.* **32**, 241–274.
- Prosperetti, A. and Oguz, H. N.** (1993). The impact of drops on liquid surfaces and the underwater noise of rain. *Annu. Rev. Fluid Mech.* **25**, 577–602.
- Rowe, L.** (1994). The costs of mating and mate choice in water striders. *Anim. Behav.* **48**, 1049–1056.
- Schilling, K. and Zessner, M.** (2011). Foam in the aquatic environment. *Water Res.* **45**, 4355–4366.
- Spence, J. R.** (1981). Experimental analysis of microhabitat selection in water-striders (Heteroptera: Gerridae). *Ecology* **62**, 1505–1514.
- Spence, J. R. and Andersen, N. M.** (1994). Biology of water striders: interactions between systematics and ecology. *Annu. Rev. Entomol.* **39**, 101–128.
- Tsimplis, M. N.** (1992). The effect of rain in calming the sea. *J. Phys. Oceanogr.* **22**, 404–412.
- Vepsäläinen, K. and Jarvinen, O.** (1974). Habitat utilization of *Gerris argentatus* (Het. Gerridae). *Ent. Scand.* **5**, 189–195.
- Walker, J. A.** (1998). Estimating velocities and accelerations of animal locomotion: a simulation experiment comparing numerical differentiation algorithms. *J. Exp. Biol.* **201**, 981–995.
- Walls, P. L. L., Bird, J. C. and Bourouiba, L.** (2014). Moving with bubbles: a review of the interactions between bubbles and the microorganisms that surround them. *Integr. Comp. Biol.* **54**, 1014–1025.
- Wheelwright, N. T. and Wilkinson, G. S.** (1985). Space use by a Neotropical water strider (Hemiptera: Gerridae): sex and age-class difference. *Biotropica* **17**, 165–169.
- Woolf, D. K.** (2001). Bubbles. In *Encyclopedia of Ocean Sciences* (ed. J. H. Steele, S. A. Thorpe and K. K. Turekian), pp. 352–357. San Diego, USA: Academic Press.
- Wu, L., Lian, Z., Yang, G. and Ceccarelli, M.** (2011). Water dancer II-a: a non-tethered telecontrollable water strider robot. *Int. J. Adv. Robot. Syst.* **8**, 10–17.